Phosphotungstic acid-supported melamine–terephthalaldehyde covalent organic framework as a novel and reusable nanostructured catalyst in three-component synthesis of 2H-indazolo[2,1-*b*] phthalazine-trione derivatives

Seyyed Jafar Saghanezhad[1] · Luigi Vaccaro[2] · Amanollah Zarei Ahmady[3,4] · Razieh Farsi[5]

Abstract

In this study, phosphotungstic acid ($H_3PW_{12}O_{40}$)-supported melamine–terephthalaldehyde Covalent Organic Framework (COF-PTA) has been prepared as a novel solid acid catalyst for the synthesis of 2H-indazolo[2,1-*b*]phthalazine trions under solvent-free conditions. The catalyst was characterized by X-ray diffraction (XRD), thermogravimetric analysis (TGA), Fourier-transform infrared spectroscopy (FT-IR), scanning electron microscope (SEM) and Brunauer–Emmett–Teller (BET) surface area analysis. The advantages of using this ecofriendly protocol include: excellent yield in a shorter time period, inexpensive chemicals without any use of solvents, simple experimental and work-up procedure. The catalyst was readily separated and was recycled for several runs with no significant loss of catalytic property.

✉ Amanollah Zarei Ahmady
  zarei-a@ajums.ac.ir

1   ACECR-Production Technology Research Institute, Ahvaz, Iran

2   Laboratory of Green S.O.C, Dipartimento Di Chimica, Biologia E Biotecnologie, Università Degli Studi Di Perugia, Via Elce di Sotto 8, 06123 Perugia, Italy

3   Nanotechnology Research Center, Ahvaz Jundishapur University of Medical Sciences, Ahvaz, Iran

4   Marine Pharmaceutical Science Research Center, Ahvaz Jundishapur University of Medical Sciences, Ahvaz, Iran

5   Department of Science, Faculty of Science, Technical and Vocational University (TVU), Tehran, Iran

🖄 Springer

Introduction

Today, green chemistry processes are considered due to increasing attention to environmental issues. In this regard, replacing conventional homogeneous catalysts with heterogeneous catalysts is considered as a solution. In recent years, heteropolyacids have been considered as solid acid catalysts [1–3]. These materials which are also known as polyoxometalates are strong in terms of acidity and to the extent of strong inorganic acids. In general, heteropolyacids have many applications as catalysts including oxidation–reduction properties. Heteropolyacids also possess diverse structure, high acidity, high solubility in polar and non-polar solvents, environmental compatibility and resistance to hydrolysis and heat [4–7]. The low surface area of heteropolyacids is their biggest limitation in catalytic systems [8–10].

Therefore, immobilization of heteropolyacids on solid substrates, with the aim of increasing their effective surface area, increases the catalytic efficiency of these compounds in catalytic systems [11–14]. Several materials such as activated carbon [13], mesoporous Al-SBA-15 [15], macroporous materials POM@MOF-199@LZSM-5 [16], Graphitic Carbon Nitride [17], Zirconia- [18] silica [19] γ-Al$_2$O$_3$ [20] HPA@MOF@CA [3] Hierarchical faujasite zeolite [21], Ni-MOF composite[22] among others have been used for heteropolyacids immobilization.

Covalent organic frameworks with abundant pore structure and high surface areas are a unique class of porous crystalline polymers formed by reversible covalent bonding of light elements with organic structural units [23–26]. COFs can provide promising platforms for various applications such as heterogeneous catalysis, semiconductors, and sensors due to their characteristic properties such as very high free surface area, low density, high thermal and chemical stability, and uniform cavities and high porosity [27–31]. Accordingly, it is of interest to evaluate the synergic effect of phosphotungstic acid (PTA) immobilized COF in catalysis.

On the other hand, in the last few decades, the nitrogen-containing heterocyclic compounds have been a subject of great interest due to their wide application. Indazole[2,1-*b*]phthalazine-triones are prominent N-heterocyclic phthalazine derivatives having bridgehead hydrazine heterocycle and are bioisosteres of indoles. The synthetic importance of these derivatives is due to their biological and medicinal properties such as anti-inflammatory, anti-cancer and anti-fungal [32–36].

Review of the scientific literature shows that several methods have been reported for the synthesis of 2H-indazolo [2,1-*b*] phthalazine trions such as: p-TSA [37], H$_2$SO$_4$[38], wet cyanuric chloride [39], nano-alumina sulforic acid [35], Caffeine-H$_2$SO$_4$ [40],ZrOCl$_2$ [41], Iodine[42] sulfuric acid-modified PEG-6000 [43] silica gel [44] melamine trisulfonic acid [45], cyanuric chloride[39] dodecylphosphonic acid[46] as catalysts. However, most of these methods possess disadvantages including use of expensive catalyst or solvent, long reaction time, strong acidic conditions and harsh reaction conditions. Therefore, it is necessary to provide new methods for the synthesis of these compounds.

Therefore, we decided to design a new and green method for the synthesis of 2H-indazolo [2,1-*b*] phthalazine trions through COF-PTA as a recyclable catalyst to overcome these limitations.
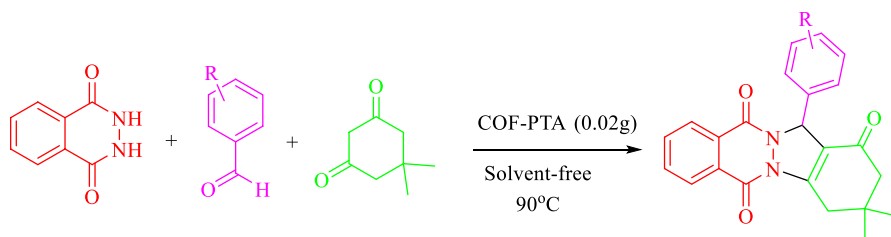
Scheme 1 One-pot preparation of 2H-indazolo[2,1-*b*]phthalazinetrion derivatives

In this study, heterogeneous catalysts were prepared by supporting phosphotungstic acid on melamine–terephthalaldehyde covalent organic framework. Then, the efficiency of these catalysts in the reaction of phthalazines was investigated and parameters such as reaction time, amount of catalyst and temperature for this reaction were optimized (Scheme 1).

Experimental

General

Chemicals were purchased from Chemical Companies with at least for synthesis grade and were used without further purification. All yields refer to isolated products. Products were characterized by comparison of their physical data such as IR, ^{1}H NMR and ^{13}C NMR spectra with authentic samples. By using TMS as an internal standard, NMR spectra were recorded in CDCl$_3$ on a Bruker Advance DPX 250 MHz spectrometer. Determination of the products' purity in the course of the reaction was monitored by TLC on silica gel polygram SILG/UV 254 plates. IR spectra were recorded on a BOMEM MB-Series 1998 FT-IR spectrophotometer as KBr disks. The melting points were recorded in open capillary tubes and were uncorrected. The SEM images and EDX-Map were recorded by TESCAN MIRA III FESEM. The BET diagrams were recorded via BELSORP MINI II.

A general procedure for the preparation of 2H-indazolo[2,1-b]phthalazine-trione derivatives catalyzed by COF-PTA nanoparticles under solvent-free conditions

In a test tube, COF-PTA (0.02 g) was added to the mixture containing dimedone (1 mmol), phthalhydrazide (1 mmol) and benzaldehyde derivatives (1 mmol). The test tuble containing the materials was heated under solvent-free conditions at 90 °C for 5–10 min. After the completion of reaction as indicated by TLC, the insoluble crude product was dissolved in dichloromethane and hot ethanol and the solid catalyst was filtered off. All the resulting products were purified and characterized by spectroscopic techniques. The crude product was purified by recrystallization from ethanol to afford the pure product.

Synthesis of melamine-based covalent organic framework (COF)

With some modifications of the first reported procedure [47], a typical solvothermal method [48] was followed for the preparation of COF. Accordingly, melamine (470 mg, 3.73 mmol) and terephthalaldehyde (750 mg, 5.59 mmol) were dissolved in DMSO (23 mL) in a Teflon-lined laboratory autoclave, which was heated at 180 °C for 14 h. Subsequently, the product was washed thoroughly, with excess acetone (30 mL×2) and dichloromethane (30 mL×2). Finally, a white powder was obtained, which was dried in an oven at 60 °C for 12 h.

Synthesis of COF-PTA

In a round-bottom-flask, melamine–terephthalaldehyde COF (1 g) was dispersed in ethanol (25 mL) and the suspension was sonicated for 10 min. Subsequently, phospho-tungstic acid (1.4 g, about 0.5 mmol) was added and the suspension was stirred for 2 h. At the end, the suspension was filtered, washed with ethanol and at last with plenty of water so that the filtrate was not acidic. Afterward, the precipitate (COF-PTA) was separated. Finally, COF-PTA was dried in the oven at 60 °C for 12 h. According to determination of pH in the NaCl solution, it was calculated that approximately 9.2 mmol H^+/g of the catalyst is present.

Spectral data for selected compounds

3,4-Dihydro-3,3-dimethyl-13-(3-flourophenyl)-2-H-indazolo[2,1-*b*]phthalazine 1,6,11(13H)-trione (Table 3, entry 7): Yield 95%, M.P.=227–229 °C. IR (KBr) (v max, cm^{-1}): 2957, 2873, 1660, 1631, 1603, 1408, 1390, 1313, 1269, 1142, 795, 775, 697.^{1}H NMR (CDCl$_3$, 250 MHz): 1.20 (s, 6H), 2.33 (s, 2H), 3.19 (AB system, dd, 1H, J=19.1 Hz and J=2.2 Hz), 3.27 (d, 1H, J=19.2 Hz), 6.31 (s, 1H), 7.00–7.10 (pt, 1H), 7.22–7.32 (m, 3H), 7.84–7.88 (m, 2H), 8.25–8.28 (m, 1H), 8.34–8.37 (m, 1H). ^{13}C NMR (CDCl$_3$, 62.5 MHz): 29.49, 29.65, 35.68, 39.02, 51.91, 65.32, 114.8, 115.2, 116.9, 119.0, 124.0, 128.7, 129.0, 129.9, 131.2, 131.3,134.7,135.6, 139.9, 152.1, 155.4, 157.0, 161.9, 165.8, 193.0.

Results and discussion

The target catalyst COF-PTA was easily synthesized according to the procedure presented in Scheme 2, and the structure confirm was characterized by spectral techniques including FTIR, XRD, SEM, EDX and TGA.
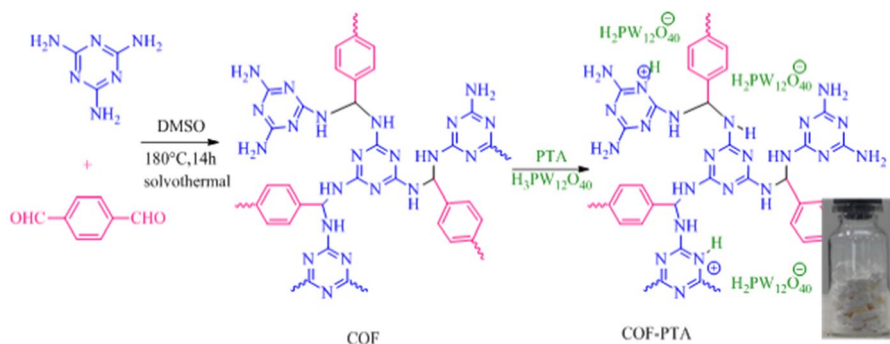
Scheme 2 Preparation of COF-PTA

Catalyst characterization

FTIR

In order to confirm the chemical structure of COF and COF-PTA, samples were analyzed by infrared spectroscopy. Figure 2 shows the FTIR spectra of the COF and COF-PTA samples produced in this study. NH bond stretching vibration at 3408 cm^{-1}, which is widely observed, is due to the presence of multiple NH bonds in the COF. Also, the peaks observed at 1548 cm^{-1} and 1474 cm^{-1} are related to stretching vibration of C=C and C=N in aromatic rings.

In COF-PTA spectrum, the presence of bands at 1080 cm^{-1} and 929 cm^{-1} was attributed to P–O and W=O stretching modes of vibrations, respectively, whereas asymmetric stretching modes of vibrations for W–O–W were present at 887 cm^{-1} (corner-sharing W–O–W) and 801 cm^{-1} (edge-sharing W–O–W), respectively. These peaks were assigned to PTA which is immobilized on the supporter COF (Fig. 1).

EDX analysis of the catalyst (Fig. 2) showed the presence of C, N, P and W elements, which confirm the obtained COF-PTA nanostructure. The amount of tungsten was also analyzed by inductively coupled plasma atomic emission spectroscopy (ICP-AES), which was 6.31%.

BET

COF and COF-PTA particles were investigated by isotherm of nitrogen uptake and desorption (BET). By this means, the pore size, pore volume, and the specific surface area of the nanoparticles were obtained. The results indicate that due to the placement of PTA groups inside the COF nanostructured cavities, the surface area of the COF-PTA is decreased to some extent. It should also be notified that the pore size of the COF nanostructures is increased after functionalization due to the change in the pore structure which is an indication of the COF flexibility. It
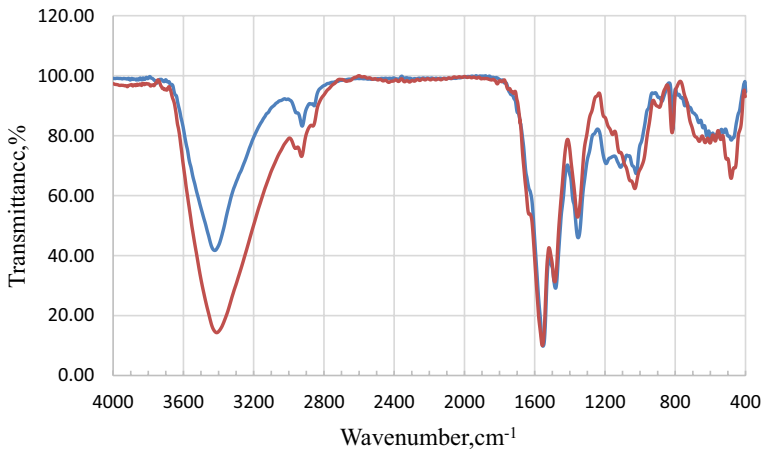
Fig. 1 FTIR spectra of **a** COF and **b** COF-PTA

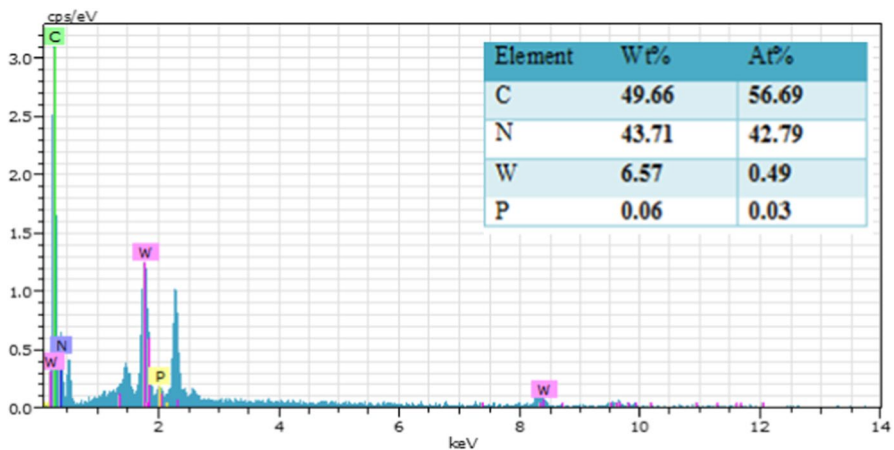| Element	Wt%	At%
C	49.66	56.69
N	43.71	42.79
W	6.57	0.49
P	0.06	0.03

Fig. 2 EDAX image of COF-PTA and corresponding quantitative EDX elemental analysis

is also worthy to mention that the BET surface area for this COF which has been reported in the literature was in the range of 254–553 m^2/g [49–57]

Nitrogen adsorption diagrams of COF and COF-PTA nanoparticles are shown in Fig. 3. The results show that due to acidification, the amount of adsorption and desorption is reduced, which can be due to the filling of the pores by the penetration of PTA.

TGA

Figure 4 shows the thermal gravimetric diagram of the COF-PTA nanostructure compared to acid-free COF in the temperature range of room-temperature to 1000 °C.
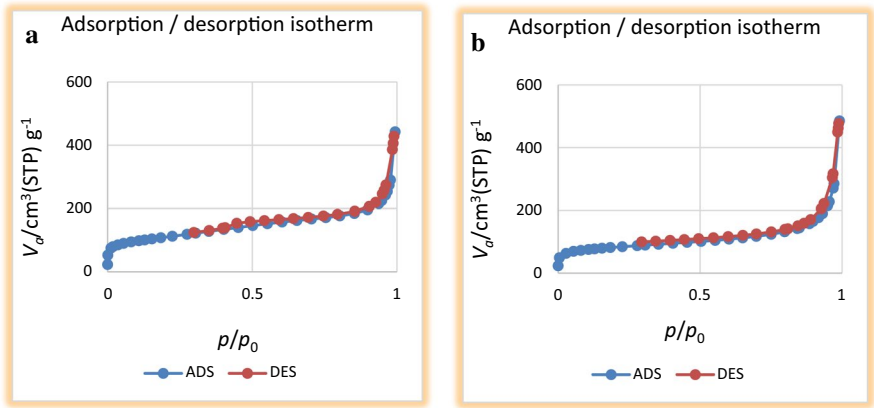
Fig. 3 The BET curve of COF (**a**); and COF-PTA (**b**)
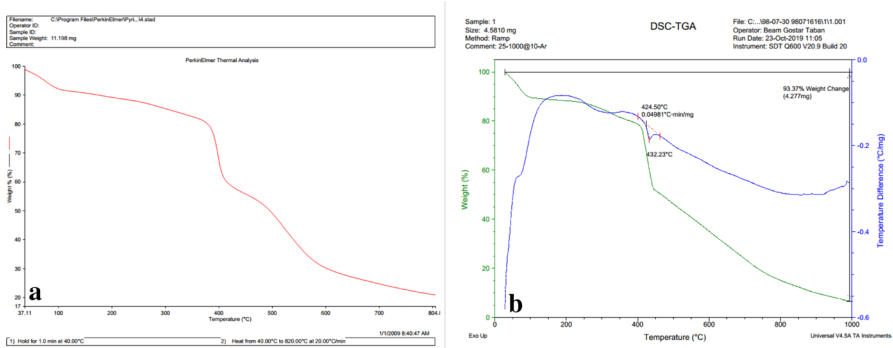

Fig. 4 The TGA curve of COF (**a**); and COF-PTA (**b**)

Thermal analysis results show that there is no structural decomposition up to 400 °C, but after that, it is the onset of weight loss which is attributed to COF polymer framework. In the COF-PTA thermometric diagram in Figure (b), the decomposition onset is started at about 424 °C, which is slightly higher than pristine COF. Accordingly we can conclude that the functionalization by PTA has increased thermal stability of the composite (Fig. 5).

To study the surface morphology of the catalyst, scanning electron microscopy (SEM) images of the catalyst were employed. As it is obvious in the SEM images, there are nanostructured appendages which are capable of increasing surface area which is beneficial for catalytic activity.
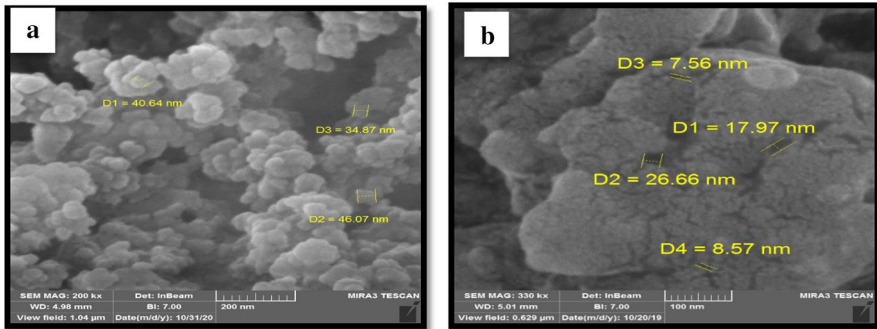
Fig. 5 SEM images of COF **(a)** and COF-PTA **(b)**

XRD

The XRD pattern of the COF-PTA was recorded (Fig. 6). Due to the high intensity of the COF peaks, the supported PTA is not very obvious. The absence of clearly defined high-intensity peaks owing to the crystalline PTA structure in the catalyst verifies the high dispersion of the heteropolyacid on the COF [58]

Catalytic activity

After determination of the structure of COF-PTA, to evaluate its efficacy as a catalyst in the promotion of the synthesis of 2H-indazolo[2,1-*b*]phthalazine-trione derivatives, the reaction between 1 mmol phthalhydrazide with 1 mmol 4-chlorobenzaldehyde, and 1 mmol dimedone, was selected under solvent-free conditions.
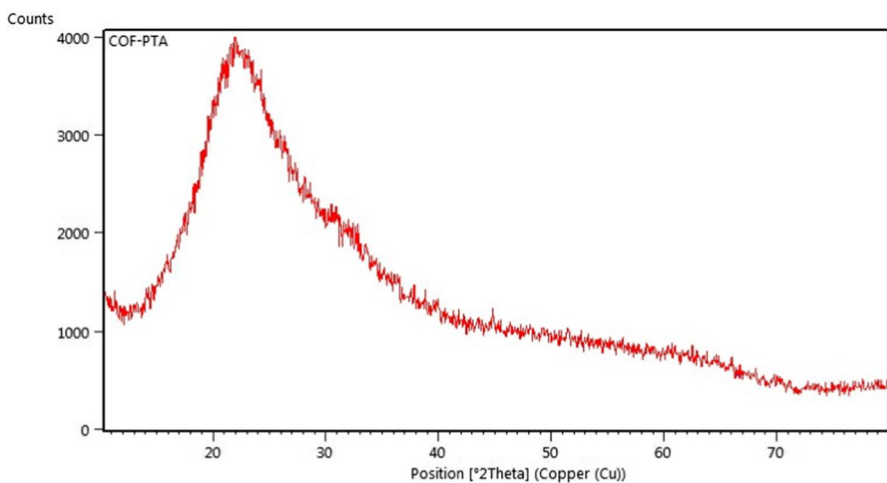

Fig. 6 XRD pattern of COF-PTA

Table 1 Surface area, average pore width and total pore volume (V_{total}) of COF and COF-PTA

Sample	BET surface area ($m^2\ g^{-1}$)	V_{total} ($cm^3 g^{-1}$)	Pore size (nm)
COF	387.35	0.6205	6.4082
COF-PTA	296.14	0.7302	9.8635

Table 2 The one-pot three component reaction of phthalhydrazide (1 mmol), dimedone (1 mmol) and benzaldehyde (1 mmol) under different conditions

Entry	Catalyst (g)	Temperature (°C)	Time (min)	Yield %
1	–	100	60	–
2	0.01	100	20	78
3	0.02	90	5	95
4	0.02	100	5	95
5	0.02	80	40	78
6	0.02	25	60	–
7	0.02	60	60	35

Initially, we continued our efforts to identify the most suitable reaction conditions for the synthesis of 2H-indazolo[2,1-*b*]phthalazine trions.

The effect of various parameters, such as reaction temperature, amount of catalyst and reaction time on the reaction of the model, was investigated. The basis of the results tabulated in Table 1 (Entry 4), when the reaction was performed at 90 °C in the presence of COF-PTA 0.02 g, excellent performance was achieved in a short reaction time.

Afterward, in order to evaluate the efficiency of this protocol, the generality of this reaction was investigated using several types of aldehydes containing electron-donating and electron-withdrawing groups.

In all cases, the reactions showed the corresponding products with good to excellent yield (Table 2).

Afterwards, in order to evaluate the efficiency of this protocol, the generality of this reaction was investigated using several types of aldehydes containing electron-donating and electron-withdrawing groups.

In all cases, the reactions showed the corresponding products with good to excellent yield (Table 3).

The most important feature that should be considered in the field of practical application of heterogeneous systems is the half-life of the catalyst and its recyclability. To evaluate the catalytic capacity of recycled catalysts, after the reaction of phthalhydrazide and dimedone for the first time, which led to the formation of the product with 90% efficiency, the catalyst was separated from the reaction mixture and after washing with dichloromethane, and dried in an oven at 90 °C for 30 min, tested his activity in the next performance. The results in Fig. 7 show that the catalyst can be used for at least four cycles with only a slight reduction in catalytic activity.

Table 3 Synthesis of 2H-indazolo [2,1-*b*] phthalazine trions derivatives in the presence of COF-PTA as the catalyst
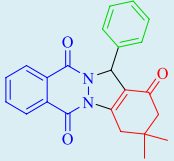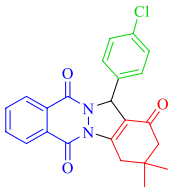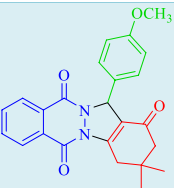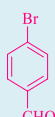
Entry	Aldehyde	Product	Time (min)	Yield (%)	Melting point (°C) Found	Melting point (°C) Lit
1	CHO		5	95	208–210	207–209[59]
2	Cl CHO		5	96	261–263	262–264[60]
3	OCH₃ CHO		20	89	220–222	218–220[60]
4	CH₃ CHO		5	94	227–229	227–229[61]
5	Br CHO		5	96	264–266	264–267[61]
6	NO₂ CHO		5	97	222–223	220–222[61]
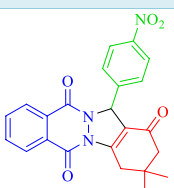
Table 3 (continued)
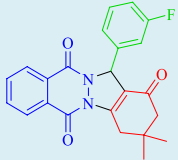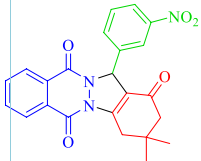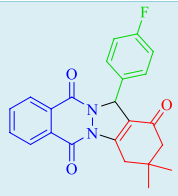
7	3-F C₆H₄ CHO (structure)	product (structure)	15	95	227-229	228-230[62]
8	2-NO₂ C₆H₄ CHO (structure)	product (structure)	10	89	268-270	270-272[63]
9	4-F C₆H₄ CHO (structure)	product (structure)	10	95	217-219	217-219[63]
10	2-NO₂ C₆H₄ CHO (structure)	product (structure)	10	87	233-235	234-236[64]
11	2-Cl C₆H₄ CHO (structure)	product (structure)	15	92	266-268	264-266[64]
12	2,5-Cl₂ C₆H₃ CHO (structure)	product (structure)	10	90	219-221	219-221[64]

Finally, to demonstrate the merits of this method, we compared our catalyst with some of the other catalysts reported in the literature. The model reaction of dimedone, phthalhydrazide and benzaldehyde was considered as a representative example. It is clear from Table 4 that the results of our method in this paper are superior to most of the previously reported methods in terms of catalyst amount,
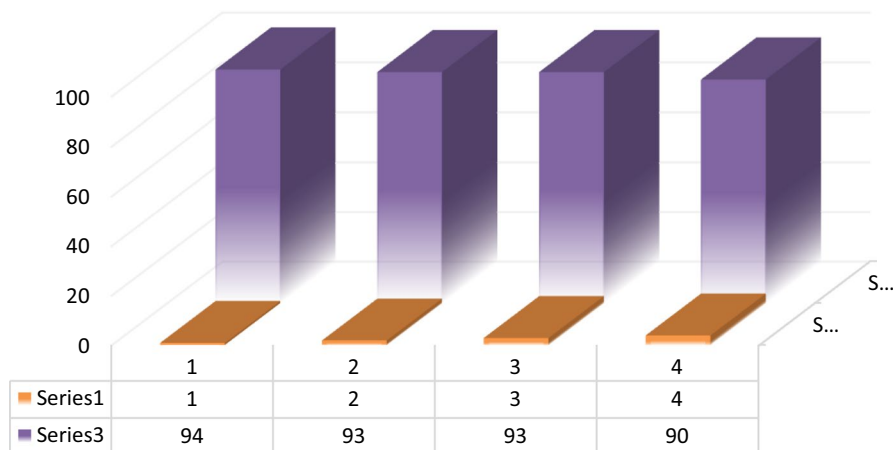
Fig. 7 Reusability of the catalyst

Table 4 Comparison of catalytic activity of COF-PTA nanostructures with some other catalysts in the reaction of dimedone, phthalhydrazide and benzaldehyde

Entry	Catalyst used	Reaction conditions	Time (min)	Yield (%)	Catalyst loading	References
1	Nano-alumina sulforic acid	Neat/110 °C	15	72	0.04 mg	[35]
2	Fe_3O_4@Silica sulfuric acid	Solvent free, 100 °C	35	88	0.075 g	[65]
3	PMA–SiO_2	Solvent free, 80 °C	30	85	0.05 mmol%	[66]
4	$[Simp]_3PW_{12}O_{40}$	Solvent free, 80 °C	20	85	0.03 g	[67]
5	MNPs-guanidine	Solvent free, 70 °C	45	93	30 mg	[68]
6	$[Simp]HSO_4$	Solvent-free/100 °C	20	83	10 mol%	[69]
7	Polymer supported sulfonic acid	Glycerol/80 °C	55	80	30 mol%	[70]
8	COF-PTA	Solvent-free, 90 °C	5	95	18.4 mol%	This work

reaction time, isolated yields and application of available and inexpensive starting compounds for the preparation of the catalyst.

A plausible reaction mechanism for the synthesis of 2H-indazolo[2,1-*b*] phthalazinetrione, in the presence of the COF-PTA catalyst, is depicted in Scheme 3. Initially, the reaction between dimedone and aldehyde occurs through Knoevenagel condensation, which is facilitated by the activation of the carbonyl group by the COF-PTA catalyst, intermediate (3) is produced. Then, Michael addition of phthalhydrazide to the C=C bond of compound (3) generates the intermediates (5), followed by cyclization which affords the corresponding product (6).
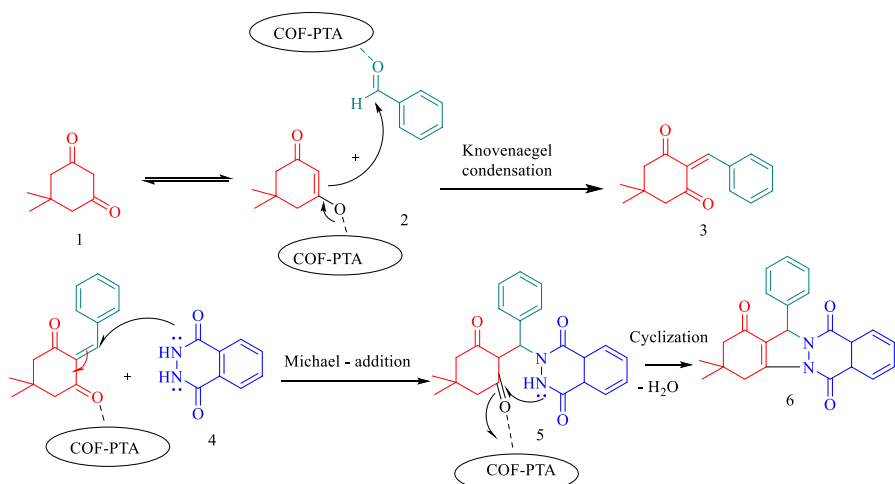
Scheme 3 Proposed mechanism of COF-PTA-catalyzed synthesis

Conclusion

In the present study, COF-PTA was successfully reported as a novel, effective and low cost nonporous catalyst for the synthesis of 2H-indazolo [2,1-b] phthalazine trions derivatives. The as-synthesized catalyst was confirmed by FT-IR, TGA, SEM, XRD, BET, and EDX techniques. This eco-friendly method offers advantages including: reusability of the catalyst, solvent-free and mild reaction conditions, good to excellent yields of products, ease of separation of product, simple experimental and work-up procedure.

Authors contributions Seyyed Jafar Saghanezhad contributed to conceptualization, methodology, validation, writing and editing the manuscript. Luigi Vaccaro contributed to methodology, validation, editing and supervision. Amanollah Zarei Ahmady contributed to conceptualization, methodology, validation, supervision, editing the final draft. Razieh Farsi contributed to experimental work assistance, writing original draft.

Declaration

References

1. J.B. Zimmerman, P.T. Anastas, H.C. Erythropel, W. Leitner, Science **367**, 397 (2020)

2. V. Polshettiwar, R.S. Varma, Green. Chem. **12**, 743 (2010)
3. J. Li, Z. Yang, G. Hu, J. Zhao, Chem. Eng. J. **388**, 124388 (2020)
4. F. Esmi, V. B. Borugadda, A. K. Dalai, Catal. Today (in press)
5. M.M. Heravi, S. Sadjadi, J. Iran. Chem. Soc. **6**, 1–54 (2009)
6. C.G.S. Lima, N.M. Moreira, M.W. Paixao, A.G. Correa, Curr. Opin. Green Sustain. Chem. **15**, 7 (2019)
7. B. Changmai, G. Pathak, J.M.H. Anal, L. Rokhum, Mini Rev. Org. Chem. **17**, 740 (2020)
8. M.N. Timofeeva, Appl. Catal. A: Gen. **256**, 19 (2003)
9. J. Li, Z. Yang, S. Li, Q. Jin, J. Zhao, J. Ind. Eng. Chem. **82**, 1 (2020)
10. Q. Zhang, X. Liu, T. Deng, Y. Zhang, P. Ma, Curr. Green Chem. **7**, 267 (2020)
11. N.A. Khan, B.N. Bhadra, S.H. Jhung, Chem. Eng. J. **334**, 2215 (2018)
12. L. Chen, B. Nohair, D. Zhao, S. Kaliaguine, ChemCatChem **10**, 1918 (2018)
13. R. Ghubayra, C. Nuttall, S. Hodgkiss, M. Craven, E.F. Kozhevnikova, I.V. Kozhevnikov, Appl. Catal., B. **253**, 309 (2019)
14. IVe. Kozhevnikov, K.I. Matveev, Russ. Chem. Rev. **51**, 1075 (1982)
15. N. Lucas, L. Gurrala, A. Athawale, J. Porous Mater. **26**, 1335 (2019)
16. S.W. Li, R.M. Gao, W. Zhang, Y. Zhang, J.S. Zhao, Fuel **221**, 1 (2018)
17. L. Wu, S. An, Y.-F. Song, Engineering **7**, 94 (2021)
18. J. Alcañiz-Monge, B. El Bakkali, G. Trautwein, S. Reinoso, Appl. Catal. B. **224**, 194 (2018)
19. M.D. Morales, A. Infantes-Molina, J.M. Lázaro-Martínez, G.P. Romanelli, L.R. Pizzio, E. Rodríguez-Castellón, Mol. Catal. **485**, 110842 (2020)
20. A. Kurhade, A.K. Dalai, Asia-Pac. J. Chem. Eng. **13**, e2249 (2018)
21. A. Talebian-Kiakalaieh, S. Tarighi, J. Ind. Eng. Chem. **79**, 452 (2019)
22. Q. Zhang, Q. Luo, Y. Wu, R. Yu, J. Cheng, Y. Zhang, RSC. Adv. **11**, 33416 (2021)
23. H.Y. Cheng, T. Wang, Adv. Synth. Catal. **363**, 144 (2021)
24. X. Feng, X. Ding, D. Jiang, Chem. Soc. Rev. **41**, 6010 (2012)
25. C.S. Diercks, O.M. Yaghi, Science **355**, eaa11585 (2017)
26. J.L. Segura, S. Royuela, M.M. Ramos, J. Chem. Soc. Rev. **48**, 3903 (2019)
27. K. Geng, T. He, R. Liu, S. Dalapati, K.T. Tan, Z. Li, S. Tao, Y. Gong, Q. Jiang, D. Jiang, Chem. Rev. **120**, 8814 (2020)
28. S. Kandambeth, K. Dey, R. Banerjee, J. Am. Chem. Soc. **141**, 1807 (2018)
29. J.L. Segura, M.J. Mancheño, F. Zamora, Chem. Soc. Rev. **45**, 5635 (2016)
30. S. Dalapati, S. Jin, J. Gao, Y. Xu, A. Nagai, D. Jiang, J. Am. Chem. Soc. **135**, 17310 (2013)
31. R. Farsi, M.K. Mohammadi, S.J. Saghanezhad, Res. Chem. Intermed. **47**, 1161 (2021)
32. G.M. Ziarani, F. Mohajer, R. Moradi, P. Mofatehnia, Curr. Org. Synth. **16**, 953 (2019)
33. N. Demirbas, A. Demirbas, Curr. Org. Catal. **8**, 27 (2021)
34. F. Masihpour, A. Zare, M. Merajoddin, A. Hasaninejad, J. Chem. Technol. Metall. **54**, 23 (2019)
35. A.R. Kiasat, S. Noorizadeh, M. Ghahremani, S.J. Saghanejad, J. Mol. Struct. **1036**, 216 (2013)
36. A. Kiasat, A. Mouradezadegun, S.J. Saghanezhad, J. Serbian Chem. Soc. **78**, 469 (2013)
37. R. Ghahremanzadeh, G.I. Shakibaei, A. Bazgir, Synlett **2008**, 1129 (2008)
38. J.M. Khurana, D. Magoo, Tetrahedron Lett. **50**, 7300 (2009)
39. X. Wang, W.W. Ma, L.Q. Wu, F.L. Yan, J. Chin. Chem. Soc. **57**, 1341 (2010)
40. S.J. Saghanezhad, S. Sayyahi, Res. Chem. Intermed. **43**, 2491 (2017)
41. H.R. Tavakoli, S.M. Moosavi, A. Bazgir, J. Korean. Chem. Soc. **57**, 472 (2013)
42. A. Varghese, A. Nizam, R. Kulkarni, L. George European, J. Chim. **4**, 132 (2013)
43. A. Hasaninejed, M.R. Kazerooni, A. Zare, Catal. Today. **196**, 148 (2012)
44. G. Krishnamurthy, K. Jagannath, J. Chem. Sci. **125**, 807 (2013)
45. W. Scheeren, Bulg. Chem. Commun. **45**, 64 (2013)
46. M. Kidwai, A. Jahan, R. Chauhan, N.K. Mishra, Tetrahedron Lett. **53**, 1728 (2012)
47. M.G. Schwab, B. Fassbender, H.W. Spiess, A. Thomas, X. Feng, K. Mullen, J. Am. Chem. Soc. **131**, 7216 (2009)
48. X. Zhao, N. Yan, RSC Adv. **5**, 69955 (2015)
49. M. Shunmughanathan, P. Puthiaraj, K. Pitchumani, ChemCatChem **7**, 666 (2015)
50. J. Ge, J. Xiao, L. Liu, L. Qiu, X. Jiang, J. Porous Mater. **23**, 791 (2016)
51. Y. Zhuang, H. Shan, Z. Zhang, S. Li, Q. Zhu, Z. Si, S. Yang, Z. Yang, D. Cai, P. Qin, Dyes Pigm. **192**, 109421 (2021)
52. Z. Li, Y. Zhi, Y. Ni, H. Su, Y. Miao, S. Shan, Polymer **217**, 123434 (2021)
53. B. He, W.-C. Li, A.-H. Lu, J. Mater. Chem. A. **3**, 13920 (2015)

54. M. Senthilkumaran, C. Saravanan, P.M. Mareeswaran, Mater. Today: Proc. **40**, 5117 (2021)
55. L. You, K. Xu, G. Ding, X. Shi, J. Li, S. Wang, J. Wang, J. Mol. Liq. **320**, 114456 (2020)
56. M. Pakizeh, P. May, M. Matthias, M. Ulbricht, J. Appl. Polym. Sci. **137**, 49595 (2020)
57. Y. Liu, H. Ou, S. Li, Q. You, H. Liu, G. Liao, D. Wang, J. Environ. Sci. **78**, 215 (2019)
58. K.V. Avramidou, F. Zaccheria, S.A. Karakoulia, K.S. Triantafyllidis, N. Ravasio, Mol. Catal. **439**, 60 (2017)
59. C.S. Maheswari, C. Shanmugapriya, K. Revathy, A. Lalitha, J. Nanostruct. Chem. **7**, 283 (2017)
60. N. Iravani, M. Keshavarz, A. Parhami, Res. Chem. Intermed. **45**, 5045 (2019)
61. J. Albadi, M. Jalali, A. Momeni, Res. Chem. Intermed. **44**, 2395 (2018)
62. M. Esmaeilpour, J. Javidi, F.N. Dodeji, S. Zahmatkesh, Res. Chem. Intermed. **47**, 2629 (2021)
63. F. Arian, M. Keshavarz, H. Sanaeishoar, N. Hasanzadeh, J. Mol. Struct. **1229**, 129599 (2021)
64. S. Karhale, V. Helavi, S.N. Appl, Sci. **2**, 1227 (2020)
65. A.R. Kiasat, J. Davarpanah, J. Mol. Catal. A: Chem. **373**, 46 (2013)
66. G. Sabitha, C. Srinivas, A. Raghavendar, J.S. Yadav, Helv. Chim. Acta. **93**, 1375 (2010)
67. R. Tayebee, M.F. Abdizadeh, B. Maleki, E. Shahri, J. Mol. Liq. **241**, 447 (2017)
68. B. Atashkar, A. Rostami, H. Gholami, B. Tahmasbi, Res. Chem. Intermed. **41**, 3675 (2015)
69. R. Tayebee, M. Jomei, B. Maleki, M.K. Razi, H. Veisi, M. Bakherad, J. Mol. Liq. **206**, 119 (2015)
70. A. Mulik, D. Chandam, P. Patil, D. Patil, S. Jagdale, S. Sankpal, M. Deshmukh, J. Heterocycl. Chem. **52**, 931 (2015)